



THE UNIVERSITY *of* EDINBURGH

Edinburgh Research Explorer

## Ordering Dimensions with Nested Dropout Normalizing Flows

**Citation for published version:**

Bekasovs, A & Murray, I 2020, 'Ordering Dimensions with Nested Dropout Normalizing Flows', Paper presented at ICML Workshop on Invertible Neural Networks, Normalizing Flows, and Explicit Likelihood Models 2020, Virtual workshop, 13/07/20 - 13/07/20.  
<[https://invertibleworkshop.github.io/accepted\\_papers/pdfs/14.pdf](https://invertibleworkshop.github.io/accepted_papers/pdfs/14.pdf)>

**Link:**

[Link to publication record in Edinburgh Research Explorer](#)

**Document Version:**

Peer reviewed version

**General rights**

Copyright for the publications made accessible via the Edinburgh Research Explorer is retained by the author(s) and / or other copyright owners and it is a condition of accessing these publications that users recognise and abide by the legal requirements associated with these rights.

**Take down policy**

The University of Edinburgh has made every reasonable effort to ensure that Edinburgh Research Explorer content complies with UK legislation. If you believe that the public display of this file breaches copyright please contact [openaccess@ed.ac.uk](mailto:openaccess@ed.ac.uk) providing details, and we will remove access to the work immediately and investigate your claim.



---

# Ordering Dimensions with Nested Dropout Normalizing Flows

---

Artur Bekasov<sup>1</sup> Iain Murray<sup>1</sup>

## Abstract

The latent space of normalizing flows must be of the same dimensionality as their output space. This constraint presents a problem if we want to learn low-dimensional, semantically meaningful representations. Recent work has provided compact representations by fitting flows constrained to manifolds, but hasn't defined a density off that manifold. In this work we consider flows with full support in data space, but with ordered latent variables. Like in PCA, the leading latent dimensions define a sequence of manifolds that lie close to the data. We note a trade-off between the flow likelihood and the quality of the ordering, depending on the parameterization of the flow.

## 1. Introduction

Normalizing flows provide a way to parameterize complex distributions in high-dimensional spaces via a sequence of invertible transformations of a simple base distribution. Unlike most other popular flexible generative models (e.g. Kingma & Welling, 2014; Goodfellow et al., 2014; Du & Mordatch, 2019), flows have a tractable likelihood, which simplifies training and model comparison. It is also easier to use tractable representations of distributions in other models and algorithms, such as for variational autoencoder (VAE) priors and posteriors.

However, generative models are not just used for estimating probabilities; we also fit these models to learn representations for down-stream tasks (Bengio et al., 2013). The latent spaces learned by normalizing flows can be semantically meaningful (Dinh et al., 2017; Kingma & Dhariwal, 2018) and can be useful for down-stream applications, such as classification (Nalisnick et al., 2019).

For standard flows the latent dimensionality must match the input dimensionality, in order to satisfy the invertibility

---

<sup>1</sup>School of Informatics, University of Edinburgh, UK. Correspondence to: Artur Bekasov <artur.bekasov@ed.ac.uk>.

constraint. This constraint presents a limitation for representation learning, where we are often interested in learning lower-dimensional representations (i.e. manifolds) that capture high-level semantic concepts (Bengio et al., 2013).

When data is constrained to a known manifold, it is possible to build a valid tractable flow on that space (Gemici et al., 2016; Rezende et al., 2020). For data without strict constraints, Kumar et al. (2020) and Brehmer & Cranmer (2020) fit an invertible flow defined on a low-dimensional manifold, and bring the manifold close to the data by minimizing square error. Neither of these methods provide a tractable probabilistic model in the data space.

In this work we maintain a full-dimensional flow, but aim to order the latent variables, such that taking the first  $K$  of them will reconstruct data with small square error. For a linear flow, our approach implements Principal Components Analysis (PCA). We encode this principle with an additional loss based on *nested dropout* (ND, Rippel et al., 2014). We show that our models successfully learn low dimensional representations, while obtaining similar likelihoods to standard flows. However, we find that the parameterization of the flow influences the representations, and we must make a trade-off between the compactness of representations and the likelihood of the flow. We hope that these findings will motivate research into flows that more naturally represent low-dimensional structure.

## 2. Nested dropout

Nested dropout was introduced by Rippel et al. (2014) in the context of autoencoders, with a goal of imposing an ordering on representation dimensions. For a linear autoencoder, nested dropout fits PCA. In a non-linear case, the learned ordering was shown to be useful for efficient retrieval and adaptive compression.

As in dropout (Srivastava et al., 2014): nested dropout randomly “drops” (i.e. zeros out) representation dimensions during training. However, rather than dropping features independently, we sample an index  $k \sim p_k(\cdot)$ , and drop dimensions  $k + 1 \dots K$ , i.e. all dimensions above that index, assuming  $K$  is the latent dimensionality.

We define  $\mathbf{z}_{\downarrow k}$  as a representation  $\mathbf{z}$  where all the dimensions above  $k$ -th have been dropped, as described above. We then

define a low-dimensional reconstruction of a given datapoint  $\mathbf{x}$  for a given index  $k$  as

$$\hat{\mathbf{x}}_{\downarrow k} = g_{\theta}(f_{\theta}(\mathbf{x})_{\downarrow k}), \quad (1)$$

where  $f_{\theta}$  and  $g_{\theta}$  are the encoder and the decoder respectively, with parameters  $\theta$ .

To train the autoencoder for a given dataset  $\{\mathbf{x}_n\}_{n=1}^N$ , we minimize the following objective:

$$\mathcal{L}(\theta) = \frac{1}{N} \sum_{n=1}^N \mathbb{E}_{k \sim p_k} [d(\mathbf{x}_n, \hat{\mathbf{x}}_{n \downarrow k})], \quad (2)$$

where  $d$  is the chosen distance metric, typically  $L_2$  distance. This set-up encourages the auto-encoder to put more information into dimensions that correspond to smaller  $k$  indices.

Rippel et al. used a geometric distribution for  $p_k$ , traditionally parameterized as  $p_k(k) = (1-p)^{k-1}p$  for a given Bernoulli probability  $p$ . We follow their choice in this work.

### 2.1. Normalizing flows with nested dropout

We start with the standard training objective of a normalizing flow. For a given parametric invertible function  $f_{\theta}$  and a base density  $\pi$ , the density of a given datapoint  $\mathbf{x}$  is:

$$p_{\theta}(\mathbf{x}) = \pi(f_{\theta}(\mathbf{x})) \left| \det \left( \frac{\partial f_{\theta}}{\partial \mathbf{x}} \right) \right|. \quad (3)$$

Given a dataset  $\{\mathbf{x}_n\}_{n=1}^N$ , we fit the flow parameters  $\theta$  by minimizing the negative log likelihood objective:

$$\mathcal{L}(\theta) = -\frac{1}{N} \sum_{n=1}^N \log p_{\theta}(\mathbf{x}_n). \quad (4)$$

We can redefine a lower-dimensional reconstruction, Eq. (1), for a normalizing flow by treating the invertible function  $f_{\theta}$  as the ‘‘encoder’’, and its inverse  $f_{\theta}^{-1}$  as the ‘‘decoder’’:

$$\tilde{\mathbf{x}}_{\downarrow k} = f_{\theta}^{-1}(f_{\theta}(\mathbf{x})_{\downarrow k}). \quad (5)$$

We combine Eqs. (2), (4) and (5) into a single objective, which specifies that the flow should have high likelihood, while also giving good reconstructions from low-dimensional parts of its representation:

$$\mathcal{L}(\theta) = \frac{1}{N} \sum_{n=1}^N (-\log p_{\theta}(\mathbf{x}_n) + \lambda \mathbb{E}_{k \sim p_k} [d(\mathbf{x}_n, \tilde{\mathbf{x}}_{n \downarrow k})]), \quad (6)$$

where  $\lambda$  is a hyper-parameter that balances the two losses. In line with Rippel et al. we estimate the expectation with a single Monte-Carlo sample.

The loss is similar to the one used by Brehmer & Cranmer (2020, Eq. 21), with two distinctions. First,  $k$  is sampled from  $p_k$  for each datapoint, rather than pre-set according to the desired manifold dimensionality. Second, while Brehmer & Cranmer use two separate flows, one for each part of the objective, we train a single flow for both.

Table 1. Average test log-likelihood (in nats) and reconstruction MSE when projecting down to 1 or 2 dimensions for the synthetic dataset. Mean  $\pm$  2 standard deviations over 10 different initializations. Superscript\* for models trained with nested dropout.

	LL	MSE(2)	MSE(1)
PCA	–	0.003	0.037
QR	$-0.804 \pm 0.000$	$0.240 \pm 0.053$	$0.321 \pm 0.025$
QR*	$-0.804 \pm 0.000$	$0.003 \pm 0.000$	$0.037 \pm 0.000$
LU	$-0.804 \pm 0.000$	$0.051 \pm 0.042$	$0.257 \pm 0.130$
LU*	$-0.805 \pm 0.001$	$0.008 \pm 0.007$	$0.037 \pm 0.001$

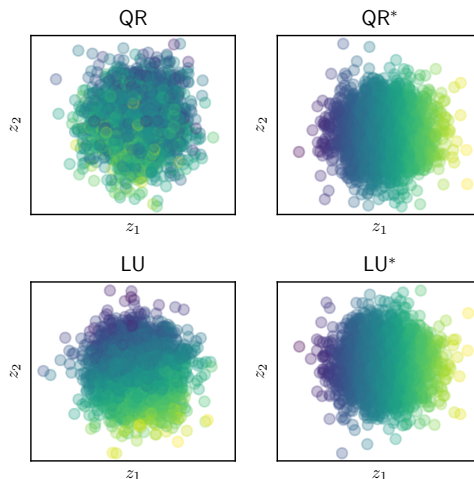


Figure 1. 2D projections  $\mathbf{z}$  of the 3D synthetic dataset, colored by the value of the first principal component of PCA. Superscript\* for models trained with nested dropout.

## 3. Experiments

### 3.1. Synthetic dataset

As a simple test case, we sample data from a centered 3-dimensional normal distribution that is scaled along the axis and then rotated. The eigenvalues of the covariance are 1, 0.1, and 0.01, so the target distribution looks like a fuzzy elliptical disc embedded into 3 dimensions. We sample  $10^4$  points for training, and another  $10^4$  points for evaluation.

We use a simple flow with a standard normal base distribution and a single invertible linear transformation. Such a flow can express the target distribution by learning to scale/rotate the base distribution as necessary. However, due to the spherical symmetry of the base distribution, the likelihood is invariant to permuting the dimensions (or any orthogonal transformation) of the base distribution.

The invertible linear transformation is parameterized by either an LU decomposition with a random, fixed permutation matrix  $\mathbf{P}$  (Kingma & Dhariwal, 2018), or a QR decomposition (Hoogeboom et al., 2019) with the orthogonal matrix parameterized by 3 Householder transformations (Tomczak

& Welling, 2016). We train the flow using the Adam optimizer (Kingma & Ba, 2015) for  $30 \times 10^3$  iterations with a batch size of 500. We set the reconstruction coefficient to  $\lambda = 20$  for nested dropout runs, with  $p_k$  set to a geometric distribution with  $p = 0.33$ .

We use PCA as a baseline for reconstruction results, where we project onto 1 or 2 principal components. Likelihood and reconstruction results are summarized in Table 1. We visualise some of the projections in Fig. 1.

For both parameterizations the additional loss improves reconstructions from 1 or 2 dimensions. For the QR parameterization, matching PCA’s optimal representation isn’t a restriction, and the test likelihood is maintained. The results for the LU parameterization have higher variance with nested dropout. The permutation matrix  $\mathbf{P}$  is not learned, and its initialization matters.

### 3.2. Images

To evaluate the method on high-dimensional data, we fit a normalizing flow with nested dropout to Fashion-MNIST images (Xiao et al., 2017). To simplify the model architecture, we pad the images by 2 pixels on each side, giving  $32 \times 32$  or 1024-dimensional images. We use the provided test set, but split the provided training set into 50 000 training images and 10 000 validation images. We dequantize the images by adding uniform noise  $\mathbf{U} \in [0, 1)^{32 \times 32}$ .

We use a RQ-NSF (C) image flow (Durkan et al., 2019) containing 3 multi-scale levels with 4 transformation steps per level, where each step consists of an activation normalization layer, a  $1 \times 1$  convolution, and a rational-quadratic coupling transform. Residual convolutional networks with 3 blocks and 128 hidden channels parameterize the 4-bin rational-quadratic splines in the coupling transforms. We train all models for  $100 \times 10^3$  iterations, with a batch size of 256. We anneal the learning rate of the Adam optimizer from  $5 \times 10^{-4}$  down to zero according to a cosine schedule (Loshchilov & Hutter, 2017, Eq. 5).

#### 3.2.1. ORDERING IN A MULTI-SCALE ARCHITECTURE

The multi-scale architecture with variable splitting, introduced by Dinh et al. (2017) and used in RQ-NSF (C), already induces a partial ordering on variables, even without the additional nested dropout objective. Some variables undergo more transformations than others, and those undergoing more transformations are eventually transformed at “coarser scale”, i.e. by transformations conditioned on variables that are further away spatially. Dinh et al. (2017, Appendix D) demonstrate that such variables contain higher-level semantic information.

Fig. 2 demonstrates the effect of this ordering. There is a sudden drop in error after including  $\approx 250$  dimensions from

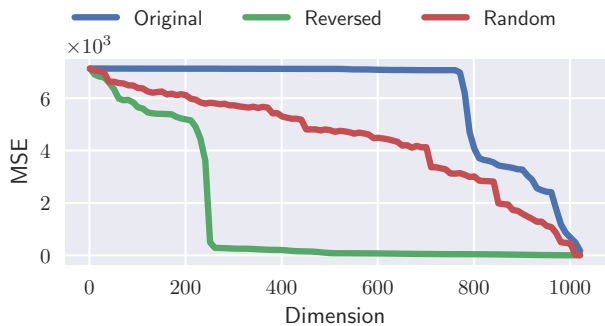


Figure 2. Mean squared error of Fashion-MNIST reconstructions for RQ-NSF (C) flow against the number of retained dimensions, varying the order in which the dimensions are dropped.

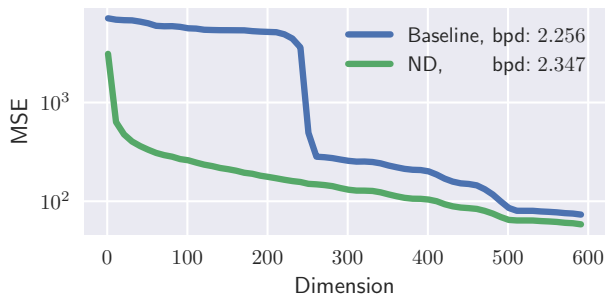


Figure 3. Mean squared error of Fashion-MNIST reconstructions for RQ-NSF (C) flow against the number of retained dimensions. Comparing a flow trained with nested dropout to the baseline without the additional loss. *bpd* is the negative test log-likelihood in bits per dimension (lower is better).

the reversed order. In our implementation of the multi-scale transform, it is this last quarter of the variables that are transformed at all 3 multi-scale levels. We use the reversed order in all further experiments, both during training with nested dropout, and during evaluation.

#### 3.2.2. TRAINING WITH NESTED DROPOUT

We now try to understand whether we can use nested dropout to improve upon the baseline RQ-NSF (C) model results in terms of reconstruction accuracy. We set the reconstruction coefficient  $\lambda = 10^{-3}$ , and we set  $p = 10^{-3}$  for the geometric distribution  $p_k$ . Reconstruction and likelihood results are shown in Fig. 3.

We note that the reconstruction curve is drastically improved, in particular for  $< 250$  dimension projections. However, we also note that the test log-likelihood of the model suffers, being reduced by  $\approx 4\%$  as a result of applying nested dropout. We hypothesize that this trade-off is controlled by the values of  $\lambda$  and  $p$ , which we explore further in Section 3.2.3.

We show samples in the ambient space and reconstructions for a baseline flow and a nested dropout flow in Fig. 4.



Figure 4. **Top:** samples from the flow. **Bottom:** reconstructions for an input image in the top left, decaying the latent dimension from 510 to 1 (left-to-right, top-to-bottom). **Left:** RQ-NSF (C) baseline. **Right:** RQ-NSF (C) with nested dropout.



Figure 5. Samples from RQ-NSF (C) trained with nested dropout. Each row shows samples with a different number of latent dimensions retained: 2, 4, 8, 16, 32, 64 for each row in order.

Even though the likelihoods of the two models differ, their samples are of comparable perceptual quality. It has been noted that the relationship between the perceptual quality of samples and likelihood is complex (Theis et al., 2016). The reconstructions demonstrate that nested dropout indeed guides the flow towards ordering the representations.

For the nested dropout flow, Fig. 5 shows samples from the flow varying the number of dropped dimensions.<sup>1</sup> Using 2 dimensions gives a generic, blurry item, which becomes sharper and more detailed given more latent features.

### 3.2.3. HYPER-PARAMETERS

We perform a limited grid-search for the  $\lambda$  and  $p$  hyper-parameters. We perturb each hyper-parameter independently, starting with the baseline values used in the previous section. Results are shown in Fig. 6.

The value of  $p$  has a limited effect on the reconstruction curve. A lower value (which causes more dimensions to be dropped on average during the run) marginally improves the MSE numbers for  $< 200$  latent dimensions.

<sup>1</sup>As noted by Brehmer & Cranmer (Section 2.C, 2020), sampling in this fashion does not correspond to sampling from densities on corresponding manifolds.

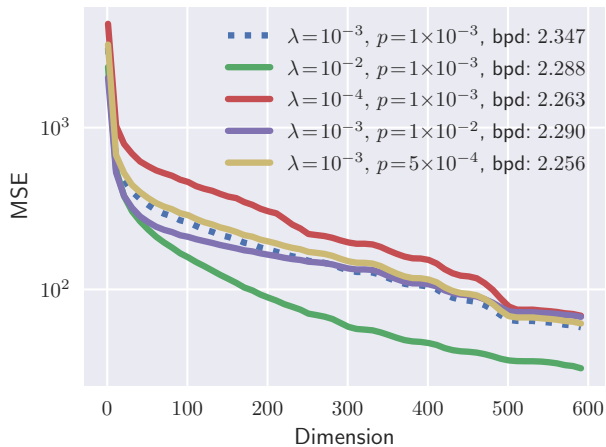


Figure 6. Mean squared error of Fashion-MNIST reconstructions for RQ-NSF (C) flow trained with nested dropout against the number of retained dimensions, varying hyper-parameters  $\lambda$  and  $p$ . The dotted line for the baseline nested dropout model.  $bpd$  is the negative test log-likelihood in bits per dimension (lower is better).

The effect of changing  $\lambda$  is more pronounced. Larger values cause a noticeable improvement in reconstruction results, while lower values have the opposite effect.

All 4 models improve upon the baseline in terms of test log-likelihood, which is surprising. There could be an interaction between  $\lambda$  and  $p$  hyper-parameters, or large variation across runs. Unfortunately, all but one result, including the one with the best reconstruction results, have slightly lower likelihoods than the standard flow.

## 4. Discussion

Nested dropout is a simple way to encourage a flow to represent data as closely as possible in the top, *principal* elements of its latent representation. Given the large redundancy in the way flows parameterize distributions, we can choose flows with similar likelihoods that provide much better low dimensional representations.

The small reduction in likelihood suggests that existing flows have some inductive bias *against* interpretable latent spaces. We also can't always apply nested dropout, because the flow must be evaluated in both directions on every iteration. For architectures with one-pass sampling, training is typically slower by a factor of two. Flows without a cheap inverse, e.g. auto-regressive flows, would be impractical.

If data really lies on a low-dimensional manifold, densities in data space are not well defined, and other work is more appropriate (Kumar et al., 2020; Brehmer & Cranmer, 2020). However, PCA is often applied when data aren't really restricted to a subspace of fixed dimensionality. We hope that nested dropout flows will be useful in similar circumstances.

## Acknowledgements

This work was supported in part by the EPSRC Centre for Doctoral Training in Data Science, funded by the UK Engineering and Physical Sciences Research Council (grant EP/L016427/1) and the University of Edinburgh.

## References

- Bengio, Y., Courville, A., and Vincent, P. Representation learning: A review and new perspectives. *IEEE Transactions on Pattern Analysis and Machine Intelligence*, 35 (8):1798–1828, 2013.
- Brehmer, J. and Cranmer, K. Flows for simultaneous manifold learning and density estimation. 2020. URL <http://arxiv.org/abs/2003.13913v1>.
- Dinh, L., Sohl-Dickstein, J., and Bengio, S. Density estimation using real NVP. In *5th International Conference on Learning Representations, ICLR 2017, Toulon, France, April 24-26, 2017, Conference Track Proceedings*. OpenReview.net, 2017. URL <https://openreview.net/forum?id=HkpbnH9lx>.
- Du, Y. and Mordatch, I. Implicit generation and generalization in energy-based models. 2019. URL <http://arxiv.org/abs/1903.08689v3>.
- Durkan, C., Bekasov, A., Murray, I., and Papamakarios, G. Neural spline flows. In Wallach, H., Larochelle, H., Beygelzimer, A., dAlché Buc, F., Fox, E., and Garnett, R. (eds.), *Advances in Neural Information Processing Systems 32*, pp. 7511–7522. Curran Associates, Inc., 2019. URL <http://papers.nips.cc/paper/8969-neural-spline-flows.pdf>.
- Gemici, M. C., Rezende, D., and Mohamed, S. Normalizing flows on Riemannian manifolds. 2016. URL <http://arxiv.org/abs/1611.02304v2>.
- Goodfellow, I. J., Pouget-Abadie, J., Mirza, M., Xu, B., Warde-Farley, D., Ozair, S., Courville, A. C., and Bengio, Y. Generative adversarial nets. In Ghahramani, Z., Welling, M., Cortes, C., Lawrence, N. D., and Weinberger, K. Q. (eds.), *Advances in Neural Information Processing Systems 27: Annual Conference on Neural Information Processing Systems 2014, December 8-13 2014, Montreal, Quebec, Canada*, pp. 2672–2680, 2014. URL <http://papers.nips.cc/paper/5423-generative-adversarial-nets>.
- Hoogeboom, E., van den Berg, R., and Welling, M. Emerging convolutions for generative normalizing flows. In Chaudhuri, K. and Salakhutdinov, R. (eds.), *Proceedings of the 36th International Conference on Machine Learning, ICML 2019, 9-15 June 2019, Long Beach, California, USA*, volume 97 of *Proceedings of Machine Learning Research*, pp. 2771–2780. PMLR, 2019. URL <http://proceedings.mlr.press/v97/hoogeboom19a.html>.
- Kingma, D. P. and Ba, J. Adam: A method for stochastic optimization. In Bengio, Y. and LeCun, Y. (eds.), *3rd International Conference on Learning Representations, ICLR 2015, San Diego, CA, USA, May 7-9, 2015, Conference Track Proceedings*, 2015. URL <http://arxiv.org/abs/1412.6980>.
- Kingma, D. P. and Dhariwal, P. Glow: Generative flow with invertible 1x1 convolutions. In Bengio, S., Wallach, H., Larochelle, H., Grauman, K., Cesa-Bianchi, N., and Garnett, R. (eds.), *Advances in Neural Information Processing Systems 31*, pp. 10215–10224. Curran Associates, Inc., 2018.
- Kingma, D. P. and Welling, M. Auto-encoding variational Bayes. In Bengio, Y. and LeCun, Y. (eds.), *2nd International Conference on Learning Representations, ICLR 2014, Banff, AB, Canada, April 14-16, 2014, Conference Track Proceedings*, 2014. URL <http://arxiv.org/abs/1312.6114>.
- Kumar, A., Poole, B., and Murphy, K. Regularized autoencoders via relaxed injective probability flow. 2020. URL <http://arxiv.org/abs/2002.08927v1>.
- Loshchilov, I. and Hutter, F. SGDR: stochastic gradient descent with warm restarts. In *5th International Conference on Learning Representations, ICLR 2017, Toulon, France, April 24-26, 2017, Conference Track Proceedings*. OpenReview.net, 2017. URL <https://openreview.net/forum?id=Skq89Scxx>.
- Nalisnick, E. T., Matsukawa, A., Teh, Y. W., Görür, D., and Lakshminarayanan, B. Hybrid models with deep and invertible features. In Chaudhuri, K. and Salakhutdinov, R. (eds.), *Proceedings of the 36th International Conference on Machine Learning, ICML 2019, 9-15 June 2019, Long Beach, California, USA*, volume 97 of *Proceedings of Machine Learning Research*, pp. 4723–4732. PMLR, 2019. URL <http://proceedings.mlr.press/v97/nalisnick19b.html>.
- Rezende, D. J., Papamakarios, G., Racanire, S., Albergo, M. S., Kanwar, G., Shanahan, P. E., and Cranmer, K. Normalizing flows on tori and spheres. 2020. URL <http://arxiv.org/abs/2002.02428v1>.
- Rippel, O., Gelbart, M. A., and Adams, R. P. Learning ordered representations with nested dropout. In *Proceedings of the 31th International Conference on Machine Learning, ICML 2014, Beijing, China, 21-26 June 2014*, volume 32 of *JMLR Workshop and*

*Conference Proceedings*, pp. 1746–1754. JMLR.org, 2014. URL <http://proceedings.mlr.press/v32/rippell14.html>.

Srivastava, N., Hinton, G., Krizhevsky, A., Sutskever, I., and Salakhutdinov, R. Dropout: A simple way to prevent neural networks from overfitting. *J. Mach. Learn. Res.*, 15(1):1929–1958, 2014. URL <http://dl.acm.org/citation.cfm?id=2627435.2670313>.

Theis, L., van den Oord, A., and Bethge, M. A note on the evaluation of generative models. In Bengio, Y. and LeCun, Y. (eds.), *4th International Conference on Learning Representations, ICLR 2016, San Juan, Puerto Rico, May 2-4, 2016, Conference Track Proceedings*, 2016. URL <http://arxiv.org/abs/1511.01844>.

Tomczak, J. M. and Welling, M. Improving variational auto-encoders using Householder flow. 2016. URL <http://arxiv.org/abs/1611.09630v4>.

Xiao, H., Rasul, K., and Vollgraf, R. Fashion-MNIST: a novel image dataset for benchmarking machine learning algorithms. 2017. URL <http://arxiv.org/abs/1708.07747v2>.